

Relationship between Mechanical and Dynamical Properties of Glass Forming Liquids<sup>†</sup>S. S. Ashwin,<sup>‡,§</sup> Y. Brumer,<sup>§,||</sup> David R. Reichman,<sup>§,⊥</sup> and Srikanth Sastry<sup>\*,‡</sup>

Theoretical Sciences Unit, Jawaharlal Nehru Centre for Advanced Scientific Research, Jakkur PO, Bangalore 560 064, India, and Department of Chemistry and Chemical Biology, Harvard University, 12 Oxford St., Cambridge, Massachusetts 02138

Received: June 30, 2004; In Final Form: October 5, 2004

We investigate the mechanical properties of several model liquids and corresponding local energy minima (inherent structures) in an attempt to explore their connection to slow dynamics and vitrification. In particular, we study the correlation between the distribution of forces between particles and the glass transition in a variety of liquids (with both attractive and repulsive interactions), including network forming liquid silicon, and silica. Such a correlation has been proposed, in analogy with granular materials, within the framework of a unified “jamming phase diagram” and has been studied for some model liquids through simulations recently. We postulate that the plateau behavior at low forces is related to the fragility of the glass former, and provide preliminary supporting evidence. We also consider the critical strain amplitude needed to cause inherent structure transitions and show that the critical strain correlates with the depth of the local energy minima and the onset of slow dynamics.

## I. Introduction

The nature of glass and the glass transition remains an unsolved problem after decades of concentrated activity.<sup>1</sup> Early theoretical notions of the glass transition centered on a sharp thermodynamic transition that underlies vitrification. Gibbs and co-workers proposed a transition to an ideal glass state that must occur at infinitely slow cooling to circumvent an “entropy crisis”, pointed out by Kauzmann, where the disordered state has a lower entropy than the crystal state of the same material.<sup>2–4</sup> This thermodynamic viewpoint underlies many analyses of the glass transition, including various recent theoretical approaches.<sup>5–7</sup>

Although precipitous thermodynamics has been invoked as an underlying driving force for the slow dynamics that eventually leads to vitrification, many theories of the glass transition rely primarily on kinetics rather than thermodynamics. The mode-coupling theory (MCT) of the glass transition explains the glass transition in terms of a nonlinear feedback mechanism.<sup>8</sup> Though the MCT equations are sensitive to structural changes that occur as a liquid is cooled, the glass transition predicted by MCT is of kinetic origin and does not involve the vanishing of the configurational entropy (essentially the logarithm of the number of unique packing configurations of particles). In models that invoke the notion of kinetic facilitation, the rapid increase of relaxation times as control parameters are changed is *entirely* the consequence of kinetics because such models have completely trivial static properties.<sup>9–12</sup> Thus, drastically different theories may separately yield compelling pictures of the underlying cause of slow dynamics in glassy systems. These pictures may be difficult to differentiate either by experiment or computer simulation. Given this state of affairs, new paradigms and organizing principles are to be welcomed.

One interesting new perspective that has been put forward is the “jamming” picture of Nagel, Liu, and co-workers<sup>13</sup> to provide a unified description of systems exhibiting structural arrest, including glass forming liquids, granular materials, colloidal systems, foams, gels, etc. Temperature and the associated thermal motion of atoms and molecules plays a significant role in the behavior of glass forming liquids, whereas temperature plays no significant role in systems such as granular materials, which are therefore termed *athermal*. In athermal systems, the parameter that determines the transition from jammed (or structurally arrested) states to fluid states is some form of external mechanical agitation, unlike glass forming liquids where temperature and density play the controlling role. Given the broad similarity of behavior, i.e., a transition from a structurally arrested state to a fluid state, there has been an attempt in recent times to formulate a common description of both thermal and athermal systems within a unified picture. In this spirit, Liu and Nagel proposed a “jamming phase diagram”<sup>13</sup> where one conceives of a single jammed domain in a phase diagram with temperature, density, and mechanical load forming independent control variables.<sup>14</sup> Indeed, within the context of glass forming liquids themselves, the influence on dynamics of applied shear stress, in addition to temperature and density changes, has been appreciated and studied for some time.<sup>15,16</sup> The jamming picture has been very useful in demonstrating the equal stature of external driving, temperature and density in controlling flow both in and out of equilibrium in glassy systems.<sup>16,17</sup>

A quantity that has been studied recently in this context is the distribution of forces acting between particles in jammed vs unjammed structures.<sup>18</sup> Initially studied for granular systems,<sup>19,20</sup> experimental and theoretical studies of three-dimensional stationary bead-packs revealed an exponential distribution at large forces, with the presence of a finite, small force peak or plateau. A simulation study of compressible granular systems showed that at low stress, the distribution of forces is exponential, whereas a change to a Gaussian distribu-

<sup>†</sup> Part of the special issue “Frank H. Stillinger Festschrift”.

<sup>\*</sup> Corresponding author. Electronic address: sastry@jncasr.ac.in.

<sup>‡</sup> Jawaharlal Nehru Centre for Advanced Scientific Research.

<sup>§</sup> Harvard University.

<sup>||</sup> Electronic address: brumer@fas.harvard.edu.

<sup>⊥</sup> Electronic address: reichman@fas.harvard.edu.

<sup>#</sup> Electronic address: ashwinss@jncasr.ac.in.

tion is seen at high stresses.<sup>21</sup> Force distributions have also been studied recently in model glass forming liquids studied by computer simulations.<sup>22–24</sup> In these studies, it was found that in equilibrated liquids, the force distribution is a featureless exponential, and the exponential nature of the distribution was rationalized in terms of the interaction potential, the behavior of the tail of the distribution argued to be more nearly exponential for inverse power law potentials with larger powers.<sup>22</sup> When the liquid falls out of equilibrium, the force distribution develops a small force peak, which is seen to present a signature of the glass transition.<sup>22</sup> In ref 23 evidence was shown of a breakdown of self-averaging in the force distributions for jammed configurations. Thus, the appearance of a plateau or peak at small forces, which marks the onset of jamming (the development of a yield stress) in a granular systems, may signal the onset of vitrification in a thermal system.<sup>22–24</sup> Interestingly, this feature would then serve as a subtle *structural* signal of the glass transition.

In this work, we investigate several aspects of the *dynamics* of supercooled liquids as they relate to jamming concepts. First, we investigate the correlation between  $P(f)$  and the onset of vitrification in a variety of systems, including simple and complex systems that involve both attractive and repulsive interactions. Because the analogy with granular systems may be less clear in complex cases, e.g., network forming systems, our study is aimed to probe the boundaries of this aspect of the jamming picture. Though we find that amorphous solids (as defined by inherent structures) always show essentially a Gaussian  $P(f)$ , in agreement with the jamming picture, the behavior in the liquid state is perhaps more complex than that originally posited by O'Hern et al. In particular, we do find examples where a plateau in  $P(f)$  may occur in the equilibrium liquid phase, and where no plateau may occur even under glassy conditions. We postulate that the prominence of the plateau behavior may be related to the fragility of the glass-former. Motivated by other aspects of the jamming picture, we qualitatively investigate the behavior of force networks in the supercooled state and investigate how the application of a shear strain disrupts local glassy states. In particular, we demonstrate that the onset of a rapid change in the depth of inherent structures (as well as the onset of nonexponential relaxation) is accompanied by a marked onset in the yielding behavior of the local packing structures.<sup>25</sup>

The paper is organized as follows: Section II provides computational details concerning the systems we study. In section III we investigate the correlation of the features of  $P(f)$  for small  $f$  with the dynamical behavior of the liquid. In section IV we study the behavior of the onset of inherent structure yielding with an applied shear deformation. In section V, we qualitatively study various connections between the behavior of inherent structures (and the transitions between them) with force distributions and force networks. Section VI contains a discussion of our results and a summary.

## II. Computational Details

We have studied the force distributions and related quantities for a number of model liquids, as described in subsequent sections. Here, the relevant computational details for each of these model liquids is briefly described. Further details are available in previously published work that are cited. The models we study are

1. The Kob–Andersen binary Lennard-Jones liquid.<sup>26</sup> Systems consisting of  $N = 256$  (204 type A and 52 type B) particles and  $N = 10000$  particles (8000 type A and 2000 type B) have

been studied. The particles interact via the Lennard-Jones (LJ) potential, with parameters  $\epsilon_{AB}/\epsilon_{AA} = 1.5$ ,  $\epsilon_{BB}/\epsilon_{AA} = 0.5$ ,  $\sigma_{AB}/\sigma_{AA} = 0.8$ ,  $\sigma_{BB}/\sigma_{AA} = 0.88$ , and  $m_B/m_A = 1$ . The LJ potential is modified with a quadratic cutoff and shifting at  $r_c^{\alpha\beta} = 2.5\sigma_{\alpha\beta}$ . The pairwise potential used is

$$V_{\alpha\beta}(r) = 4\epsilon_{\alpha\beta} \left[ \frac{\sigma_{\alpha\beta}^{12}}{r^{12}} - \frac{\sigma_{\alpha\beta}^6}{r^6} \right] - V_{\text{cut}}(r) \quad (1)$$

$$V_{\text{cut}}(r) = -4\epsilon_{\alpha\beta} \left\{ \left[ (6\sigma_{\alpha\beta}^{12}/r_{\text{c}\alpha\beta}^{12}) - (3\sigma_{\alpha\beta}^6/r_{\text{c}\alpha\beta}^6) \right] (r/r_{\text{c}\alpha\beta})^2 - 7(\sigma_{\alpha\beta}^{12}/r_{\text{c}\alpha\beta}^{12}) + 4(\sigma_{\alpha\beta}^6/r_{\text{c}\alpha\beta}^6) \right\} \quad (2)$$

The reduced density is 1.2. For  $N = 256$  the temperature range spans  $T = 0.39$  to  $T = 0.57$ , at which  $T$  the liquid is equilibrated. Out-of-equilibrium runs are also considered at  $T = 0.38$  and  $T = 0.40$ . Further details are as in refs 27 and 28. The  $N = 10000$  system is studied between  $T = 0.377$  and  $T = 0.7$ . The liquid is not in equilibrium below  $T = 0.552$ .

2. The 50:50 binary Lennard-Jones liquid studied by Schröder et al.<sup>29</sup> The system contains 251 particles of type A and 249 particles of type B interacting via a LJ potential with parameters  $\sigma_{BB}/\sigma_{AA} = 5/6$ ,  $\sigma_{AB} = (\sigma_{AA} + \sigma_{BB})/2$ , and  $\epsilon_{AA} = \epsilon_{AB} = \epsilon_{BB}$ . The masses are given by  $m_B/m_A = 1/2$ . The length of the sample is  $L = 7.28\sigma_{AA}$  (reduced density = 1.296) and the potential was cut and shifted at  $r_{\text{c}\alpha\beta} = 2.5\sigma_{\alpha\beta}$ . The form of the potential is the same as above, but with  $V_{\text{cut}} = 4\epsilon_{\alpha\beta} [\sigma_{\alpha\beta}^{12}/r_{\text{c}\alpha\beta}^{12} - \sigma_{\alpha\beta}^6/r_{\text{c}\alpha\beta}^6]$ . The temperatures range from  $T = 0.60$  to  $T = 0.69$  and the system is equilibrated at all temperatures. Further details are as in ref 29.

3. A two-dimensional soft sphere liquid with  $N = 10000$  particles.<sup>15</sup> The particles interact via the potential  $V_{\alpha\beta} = \epsilon(\sigma_{\alpha\beta}/r)^{12}$  with parameters  $\sigma_{BB}/\sigma_{AA} = 1.4$  (additive diameters) and  $m_B/m_A = 2$ . The potential is cut and shifted at  $r/\sigma_{AA} = 4.5$ . The reduced density is 0.8. The temperature range is  $T = 0.337$  to  $T = 2.54$  and the system is equilibrated at all temperatures. Further details are as in ref 15.

4. A two-dimensional polydisperse Lennard-Jones liquid.<sup>30,31</sup> The particle diameters are uniformly distributed between 0.8 and 1.2 of the average value. The number of particles is  $N = 990$  and the temperatures  $T = 0.4$  to  $T = 2.0$  and the system is equilibrated at all temperatures.

5. The Stillinger–Weber model of silicon.<sup>32,33</sup> Simulated configurations containing  $N = 512$  particles are analyzed, at zero pressure, and  $T = 1055$  K, 1070 K, and 1710 K. The Stillinger–Weber potential consists of a two- and a three-body term. The two body term has the form

$$v_2(r_{ij}) = \epsilon f_2(r_{ij}/\sigma) \quad (3)$$

$$f_2 = A(Br^{-p} - r^{-q}) \exp[(r - a)^{-1}] \quad r < a$$

$$f_2 = 0 \quad r > a \quad (4)$$

where  $\epsilon$  and  $\sigma$  are energy and length units and  $r_{ij}$  is the interparticle distance between the  $i$ th and the  $j$ th particles. The cutoff is at  $r = a$  beyond which the potential is equal to zero.

The three body term has the following form:

$$v_3(\mathbf{r}_i, \mathbf{r}_j, \mathbf{r}_k) = \epsilon f_3(\mathbf{r}_i/\sigma, \mathbf{r}_j/\sigma, \mathbf{r}_k/\sigma) \quad (5)$$

$$f_3(\mathbf{r}_i/\sigma, \mathbf{r}_j/\sigma, \mathbf{r}_k/\sigma) = h(\mathbf{r}_{ij}, r_{ik}, \theta_{jik}) + h(r_{ji}, r_{jk}, \theta_{ijk}) + h(r_{ki}, r_{kj}, \theta_{ikj}) \quad (6)$$

Here  $\theta_{ijk}$  is the angle between  $\mathbf{r}_i$  and  $\mathbf{r}_j$  subtended at the vertex  $i$ . We then have  $h$  given by

$$h(r_{ij}, r_{ik}, \theta_{jik}) = \lambda \exp[\gamma(r_{ij} - a)^{-1} + \gamma(r_{ik} - a)^{-1}] \left( \cos \theta_{jik} + \frac{1}{3} \right)^2 \quad (7)$$

The parameters defining the model are:

parameter	values
$A$	7.049556277
$B$	0.6022245584
$p$	4
$q$	0
$a$	1.8
$\lambda$	21.0
$\gamma$	1.20
$\sigma$	0.20951 nm
$\epsilon$	50 kcal/mol

The supercooled liquid silicon has been shown<sup>33</sup> recently to exhibit a liquid–liquid-phase transition, with the low-temperature liquid displaying “strong” character in the fragile–strong classification of the dynamical behavior of glass forming liquids;<sup>34</sup> fragile liquids display non-Arrhenius temperature dependence of viscosity and relaxation times, whereas strong liquids show Arrhenius temperature dependence. Further, strong liquids have been observed to exhibit strong Boson peaks;<sup>37</sup> in simulation studies a manifestation of the Boson peak has been identified<sup>38</sup> as a dip in the intermediate scattering function between the short time (“microscopic”) process and the caging plateau that precedes the  $\alpha$  relaxation. The system is equilibrated at all temperatures. Further details are given in ref 33.

6. The BKS model of silica.<sup>35,36</sup> The interatomic potential for BKS silica is given by

$$V_{ij} = q_i q_j / r_{ij} + A_{ij} \exp[-b_{ij} r_{ij}] - c_{ij} / r_{ij}^6 \quad (8)$$

with parameters

$i-j$	$A_{ij}$	$b_{ij}$	$c_{ij}$	atomic charges
O–O	1388.7730	2.76000	175.0000	$q_o = -1.2 e$
Si–O	18003.7572	4.87318	133.5381	$q_{si} = 2.4 e$

Simulations of a system containing  $N = 336$  atoms (112 silicon and 224 oxygen), in a cubic box of size 18.8 Å have been studied. Temperatures studied range from  $T = 2750$  K to  $T = 6100$  K. The liquid is equilibrated at all studied temperatures. BKS silica has been shown to display a fragile to strong crossover around  $T = 3500$  K.<sup>39</sup> Further details may be found in ref 36.

For each system we study, we calculate the set of forces between all pairs of particles present. This is straightforward in all the cases except silicon, because the interactions are pairwise additive. What we mean by pairwise forces in the case of silicon, where two-body and three-body interactions are present, is described below when we present results for silicon.

### III. Force Distributions

Figure 1a shows the force distribution for the Kob–Andersen liquid for  $N = 10000$  and a range of temperatures. The repulsive as well as attractive forces are shown, with the attractive forces on the negative axis. Focusing on the repulsive forces, it is seen that in all cases, the distribution is exponential. Figure 1b shows the force distributions for the Kob–Andersen liquid for  $N = 256$  and a range of temperatures that includes temperatures below the mode coupling temperature  $T_c = 0.435$ .<sup>26</sup> It has been shown recently that the diffusion constant shows a non-Arrhenius to Arrhenius crossover in this system across  $T =$

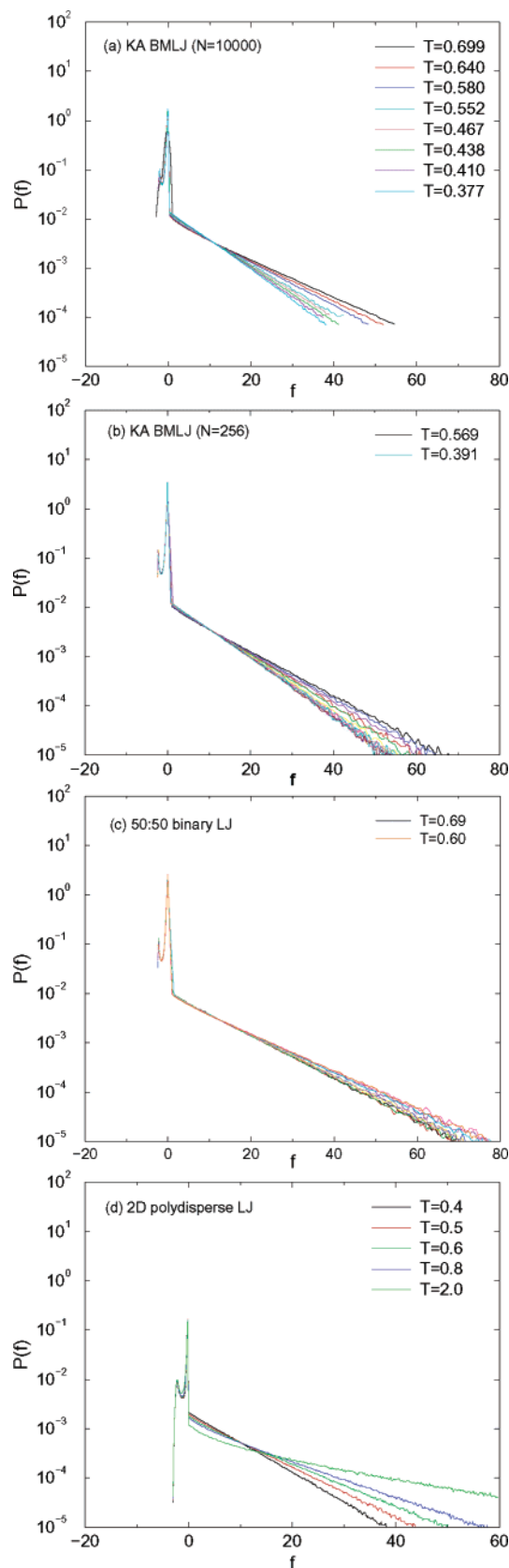


**Figure 1.** Force distribution for (a) A type particles for instantaneous configuration of the Kob–Andersen liquid for  $N = 10000$ . The liquid is not equilibrated below  $T = 0.552$ . (b) A type particles for instantaneous configuration of the Kob–Andersen liquid for  $N = 256$ . (c) A type particles for instantaneous configurations of the 50:50 binary LJ liquid for  $N = 500$ . (d) Instantaneous configurations of the two-dimensional polydisperse LJ liquid.

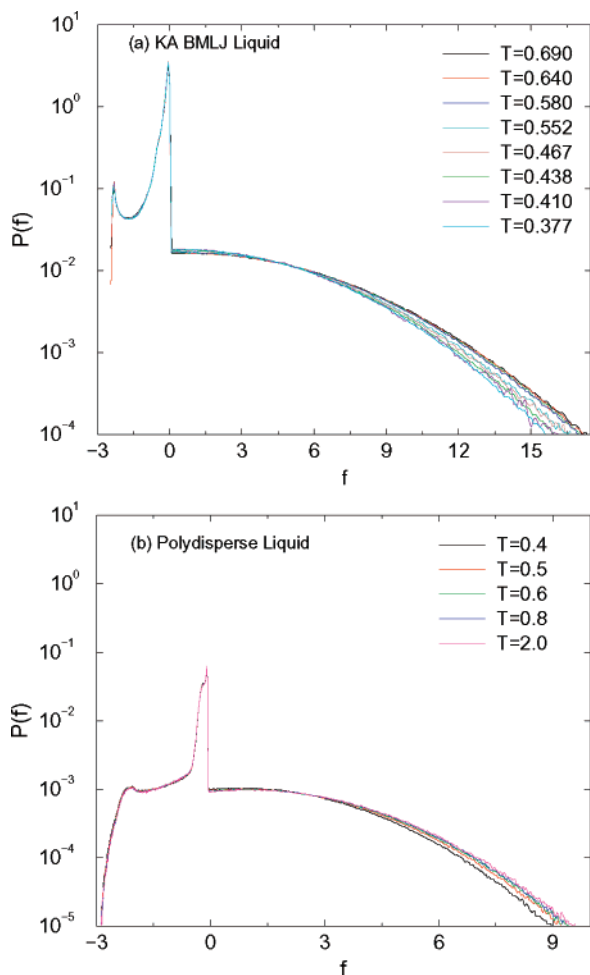


**Figure 2.** Force distribution for (a) A type particles for inherent structure configurations of the Kob–Andersen system for  $N = 10000$ . (b) Inherent structure configurations of the two-dimensional polydisperse LJ liquid.

0.435.<sup>40</sup> In this case also, the repulsive part of the force distribution is seen to be close to exponential. Indeed, for similar temperatures the force distributions for  $N = 10000$  and  $N = 256$  are very similar, and the  $N = 256$  cases have been considered simply to extend the range of temperatures studied. Figure 1c shows the force distribution for the 50:50 binary Lennard-Jones liquid which also displays exponential repulsive force distribution. The same behavior is seen in Figure 1d for the two-dimensional polydisperse LJ liquid. In all cases, the peak at zero force arises from pairs of particles at large separations, which experience weak attractive forces between them.

Next, we consider the force distributions for local energy minimum configurations or inherent structures, obtained by subjecting a sample of liquid configurations to local energy minimization. Energy minimizations are performed using steepest descent or the conjugate gradient method, and the number of configurations analyzed varies from a few tens to a few thousand configurations in the different cases analyzed. The stopping criterion for minimization is that the energy change per iteration decreases to less than 1 part in  $10^{12}$ . Figure 2a shows the force distribution for the inherent structures of the Kob–Andersen liquid with  $N = 10000$ . It is seen that the force distribution has a Gaussian form, similar to observations by Makse et al.<sup>21</sup> for  $P(f)$  above a critical value of the stress. Because local energy minima are by definition mechanically stable or jammed configurations, the observation of a Gaussian distribu-

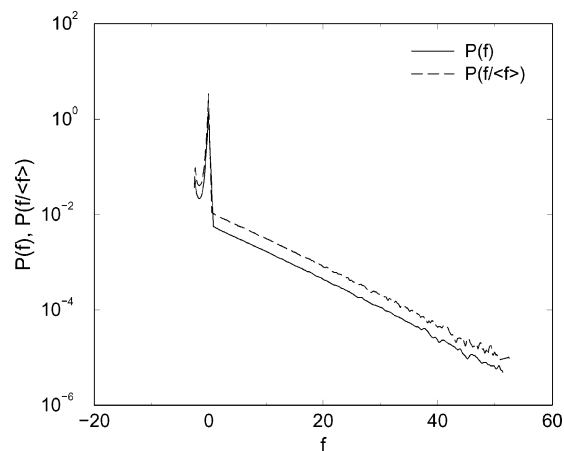


**Figure 3.** Force distribution for A type particles for instantaneous configurations of the out of equilibrium Kob–Andersen liquid, for  $N = 256$  and  $T = 0.38$ . The force distribution is calculated both (a) without normalization ( $P(f)$  in figure), and (b) normalizing to the average repulsive force for each configuration ( $P(f)/\langle f \rangle$ ) in figure). Data for (b) have been scaled by 7.454 (x axis) to match the range of curve a and shifted by 0.656 (y axis) for clarity.

tion is consistent with expectations based on previous work. Figure 2b shows the corresponding force distributions for the two-dimensional polydisperse system, which also displays Gaussian force distributions.

Although the results shown so far conform to expectations by and large, an interesting exception is the Kob–Andersen liquid at low temperatures for  $N = 10000$  where the system is not properly equilibrated, but we nevertheless observe force distributions that are similar to the cases which are well equilibrated. It should be noted that in ref 22 the glass transition is defined to occur when a threshold relaxation time of  $\tau = 1000$  (in reduced units) is reached. For all cases presented, e.g., in Figure 2b, our results are for  $T$ 's below the effective glass transition as defined by O'Hern et al. even though our system is in equilibrium. To clarify, we perform additional simulations (both constant energy and constant temperature) for 5 million time steps, quenched from a high-temperature initial run, for the Kob–Andersen liquid,  $N = 256$ , at  $T = 0.38$ . At this temperature, the system does not equilibrate for runs exceeding a few hundred million time steps, and therefore the system is clearly out of equilibrium in the 5 million time step run. Further, in view of the lack of self-averaging indicated in ref 23, we calculate the force distribution with and without normalizing the forces to the configuration-wise average of the repulsive forces. These distributions are shown in Figure 3. It is seen that the force distributions are exponential in each case. This indicates that lack of self-averaging is not an issue in this instance.

We next consider the two-dimensional binary soft sphere liquid, for which the force distributions are shown in Figure 4. In this case, as the temperature is lowered, but with the liquid still in equilibrium, a small force peak is seen to develop and is clearly visible at the lowest two temperatures. This case provides a second counterexample to expectations, because one sees a finite force peak appear in a liquid in equilibrium.

From previous results, we expect the binary soft sphere liquid to display “strong” behavior.<sup>41</sup> Such liquids have so far not been analyzed, and therefore the possibility that strong liquids exhibit force distributions that differ qualitatively from fragile liquids deserves further exploration. To this end, we consider two liquids for which evidence of strong behavior exists. The first is liquid silicon. In a recent study<sup>33</sup> of silicon using the



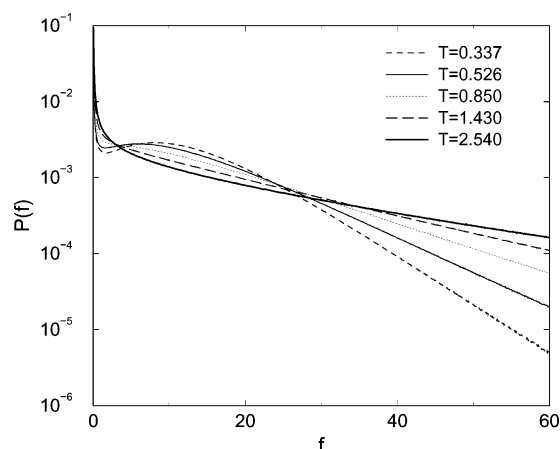


**Figure 4.** Force distribution for instantaneous configurations of the two-dimensional binary soft sphere liquid.

Stillinger–Weber potential<sup>32</sup> it has been shown that a liquid–liquid transition exists around  $T = 1060$  K and the low-temperature phase displays strong behavior, which the high-temperature phase displays fragile behavior at zero pressure. We therefore calculate the force distribution for liquid silicon at  $T = 1055$  K (below the transition),  $T = 1070$  K (above the transition), and  $T = 1710$  K (above the liquid–solid transition). Parts a–c of Figure 5 show the force distributions at these temperatures.<sup>49</sup> In each case, the distribution of nearest neighbor repulsive forces shows a Gaussian character (or a tendency to plateau), and the distribution of all forces shows a small force peak. However, the peak corresponds to neighbors farther away than the first shell, as seen by a comparison with the distribution considering the nearest neighbors alone. Therefore, in this case also, the nonexponential force distribution for small forces (or the appearance of a plateau) does not correspond to a glass transition. Further, the qualitative form of the distribution remains roughly the same (but with a growing exponential regime in the tail of the distribution at higher temperatures) at all temperatures. Thus, a sharp connection with strong behavior is also not obvious. It is likely that the nature of the distributions is related to the type of interactions that may lead to strong dynamical character in a limited temperature domain. To investigate further the role of fragility in determining the nature of the force distributions, we study liquid silica, simulated using the BKS potential.<sup>35</sup> We calculate  $P(f)$  for  $T = 2750, 3000, 3580, 4000, 4700$ , and  $6100$  K, as shown in Figure 6. BKS silica is known to have a strong to fragile transition at around  $3500$  K.<sup>39</sup> We investigate the  $P(f)$  for the repulsive parts that is Si–Si and O–O interactions. The force distributions in this case display much richer structure, reflecting the static structure of the liquid. Comparison with the nearest neighbor force distributions reveals that the largest force peak arises from nearest neighbor interactions.

The overall picture that emerges is one that is grossly consistent with that of O’Hern et al.<sup>22–24</sup> with some interesting exceptions. We have found that the LJ mixtures do not show a plateau in  $P(f)$  at small  $f$  even at temperatures where equilibration is no longer possible, whereas the soft-sphere mixture shows a plateau in the liquid phase, above  $T_c$ . Although inherent structures always display Gaussian profiles, in accordance with refs 21–24, the appearance of a plateau in  $P(f)$  may not be a sensitive measure of the location of  $T_g$ . What can one draw from the results presented in this section? It appears that there is indeed some correlation between the properties of  $P(f)$  at small  $f$  and the strong–fragile properties of the liquid. In particular, if we confine our discussion to spherical particles where the

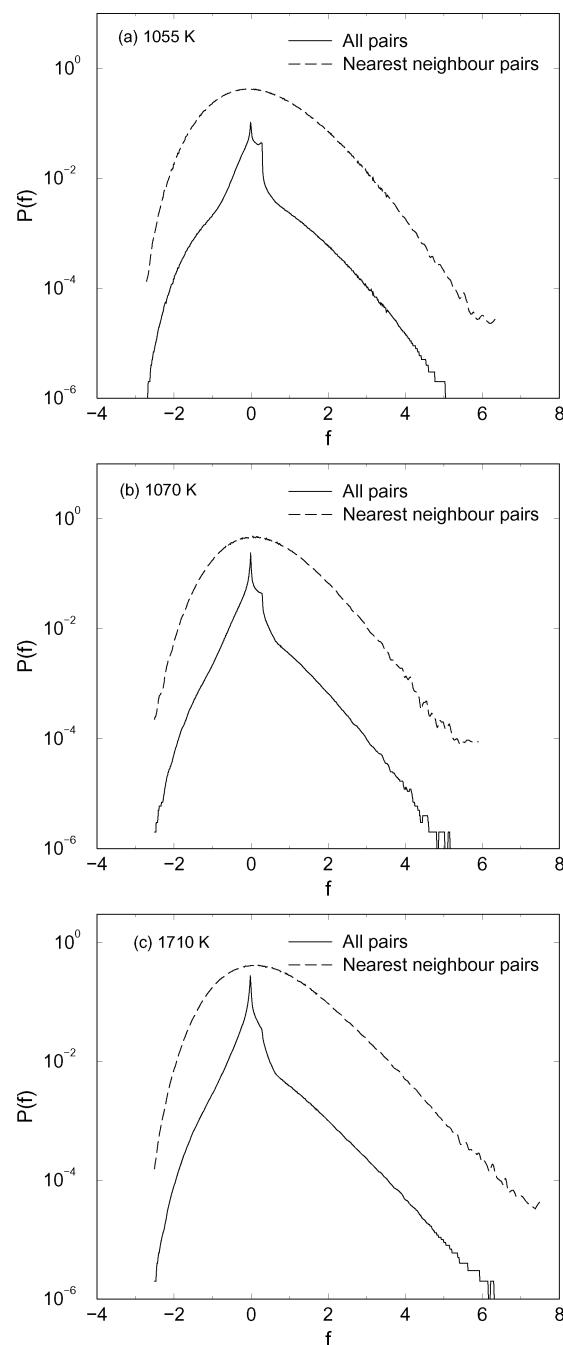


**Figure 5.** Force distribution for liquid Silicon at (a)  $T = 1055$  K, (b)  $T = 1070$  K, and (c)  $T = 1710$  K.

analogy with granular media is clearer, then we find that the appearance of a plateau at small  $f$  occurs in the case of the stronger soft sphere mixture and not in the more fragile LJ liquids.

Silicon and silica are also liquids that display a peak at low repulsive force values and are systems that may exhibit characteristics of strong liquids. It was noted above, however, that these features persist above the strong-to-fragile crossover temperatures in these systems. Given that the inherent structures of all systems show peaks in  $P(f)$  at small  $f$ , whereas instantaneous configurations may not, a useful correlation between the average number of imaginary modes (in the language of instantaneous normal modes) at a given set of thermodynamic parameters and the low  $f$  properties of  $P(f)$  may exist. Though it may be useful to pursue this connection in future work, we will argue in the next section that  $P(f)$  has some fundamental

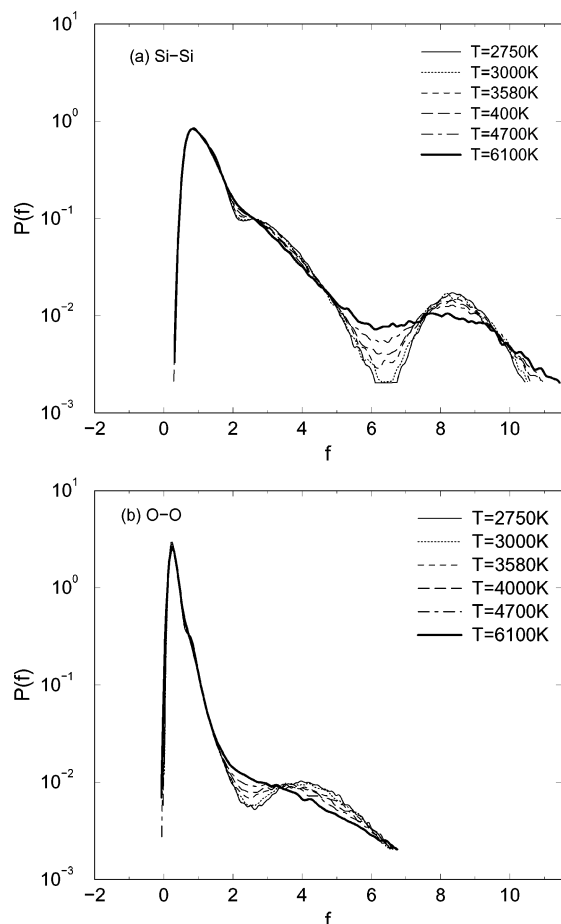


**Figure 6.** Force distribution for silica, considering all pairwise (a) Si-Si interactions and (b) O-O interactions.

limitations as an indicator of the rheological properties of a glassy system.

#### IV. Response to Deformation

To investigate other possible connections between mechanical properties of glass forming systems, and their dynamical properties, we study the response of inherent structures to shear strain deformations. For the Kob-Andersen binary LJ liquid, and the polydisperse Lennard-Jones systems with  $N = 110$  particles. Each inherent structure is subjected to a deformation given by  $x'_i = x_i + \gamma y_i$ , where  $\gamma$  is a strain variable. After such a deformation, the deformed configuration is subjected to energy minimization, and the resulting inherent structure is compared with the initial one. In each case, we determine the smallest value of  $\gamma$  that results in a transition to a new inherent structure. This critical  $\gamma$  is averaged over 1000 inherent structures for each temperature studied.

Figure 7a shows  $\gamma_c$  for the polydisperse LJ system. Although at the high temperatures  $\gamma_c$  is relatively constant, a trend toward larger values is seen at low temperatures, indicating that the inherent structures become more “robust” at low temperatures. A comparison with the average inherent structure energy vs temperature, shown in Figure 7b, indicates that the resistance to shear of the inherent structures follows that of the inherent structure energies; in particular, the increase of  $\gamma_c$  is coincident with the onset of a decrease in the inherent structure energies. It has been shown in previous work<sup>27,28</sup> that the progressive decrease of inherent structure energies marks the onset of slow dynamics in the liquid. The resistance to a shear strain deformation of the inherent structures thus also reflects the onset

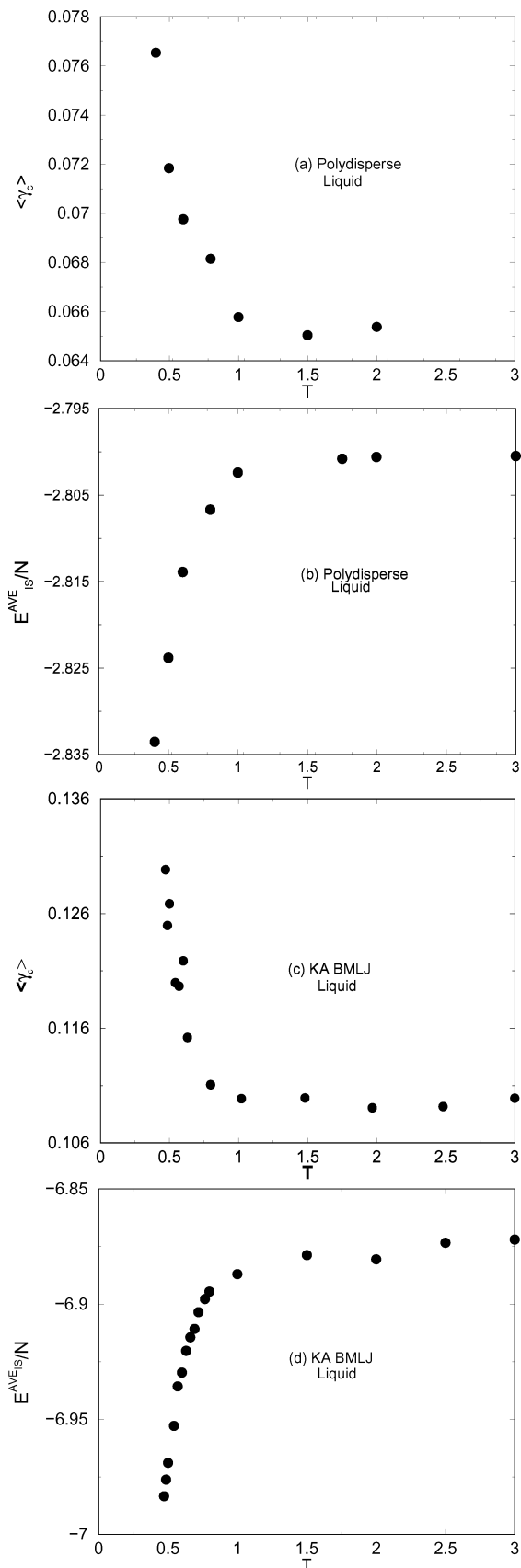


**Figure 7.** (a) Critical shear deformation  $\gamma_c$  vs temperature for the polydisperse LJ liquid. (b) The average inherent structure energy vs temperature for the polydisperse LJ liquid. (c) Critical deformation  $\gamma_c$  vs temperature for the Kob-Andersen liquid. (d) Inherent structure energy vs temperature for Kob-Andersen liquid for reduced density 1.2. of slow dynamics. Figure 7c shows  $\gamma_c$  vs temperature for the Kob-Andersen binary liquid, for which the onset temperature

has been previously estimated to be  $T_0 \sim 1.0$ .<sup>27,28</sup> It is clear that for this system as well, the behavior of  $\gamma_c$  reflects the onset of slow dynamics, and the decrease of average inherent structure energies.

What may be drawn from the results shown in Figure 7a–d? The demonstration of a sharp change in the yielding behavior of the inherent structures sampled below  $T_0$  is interesting in its own right. Taken with the results of the previous section, the data presented in Figure 7a–d suggest that some care should be taken in attempting to judge changes in mechanical behavior based on force distributions. *In particular, though the yielding behavior of the sampled inherent structures shows a rather dramatic change near  $T_0$ , the force distributions generated from the same inherent structures (the information shown in Figure 2) show only continuous and gradual changes at the temperature is lowered below  $T_0$ .*

## V. Force Networks

In the context of granular materials and models thereof, a quantity of interest has been “force chains”, which characterize the distribution of load in these jammed systems.<sup>19–21</sup> We calculate the force network for inherent structures in the polydisperse LJ liquid at  $T = 1.0$ , an example of which is shown in Figure 8a. Given the absence of a directionality to the load (provided in granular materials by gravity), we observe a two-dimensional network of forces that are more homogeneous than the corresponding liquid configuration (not shown), consistently with the observation of Makse et al.<sup>21</sup>

We next consider transitions between inherent structures and the corresponding changes in particle positions as well as forces. These are shown in Figure 8b,c for the same inherent structure transition. The particle displacements and force changes show a clear and predictable correlation, and further, illustrate the spatial extent of rearrangement involved in the inherent structure transition. A more detailed study of such transitions may be valuable in understanding spatially heterogeneous dynamics, and the emergence of a growing length scale of collective particle motions in glass forming liquids. In particular, consideration of changes in the force network may make the task of defining an associated length scale, connected to dynamic heterogeneity, simpler. In an interesting recent study, Wittmer et al. have studied force networks and the elastic properties of disordered solids.<sup>50,51</sup> They have found “soft” elastic regions of a particular average length scale exist in the inherent structure samples and that these regions are likely responsible for the anomalous vibrational properties of glasses in the terahertz frequency domain. Wittmer et al. did not study the history dependence of this length scale. Our results from this and the previous section suggest that a careful study of the length scale associated with local elasticity and local rupturing of the force network in inherent structures sampled as the temperature is lowered below known crossover temperatures ( $T_0$ ,  $T_c$ ) might be useful in understanding dynamical heterogeneity in supercooled liquids and elastic heterogeneity in glasses.

## VI. Discussion and Summary

We have studied the relationship between mechanical properties of glass forming liquids and their dynamical behavior. First, we studied force distributions in a variety of model liquids and corresponding inherent structures. Although most equilibrated atomic liquids display exponential force distributions, and inherent structures display Gaussian distributions, consistent with expectations based on previous work, we have observed some interesting exceptions. The out-of-equilibrium low-temperature

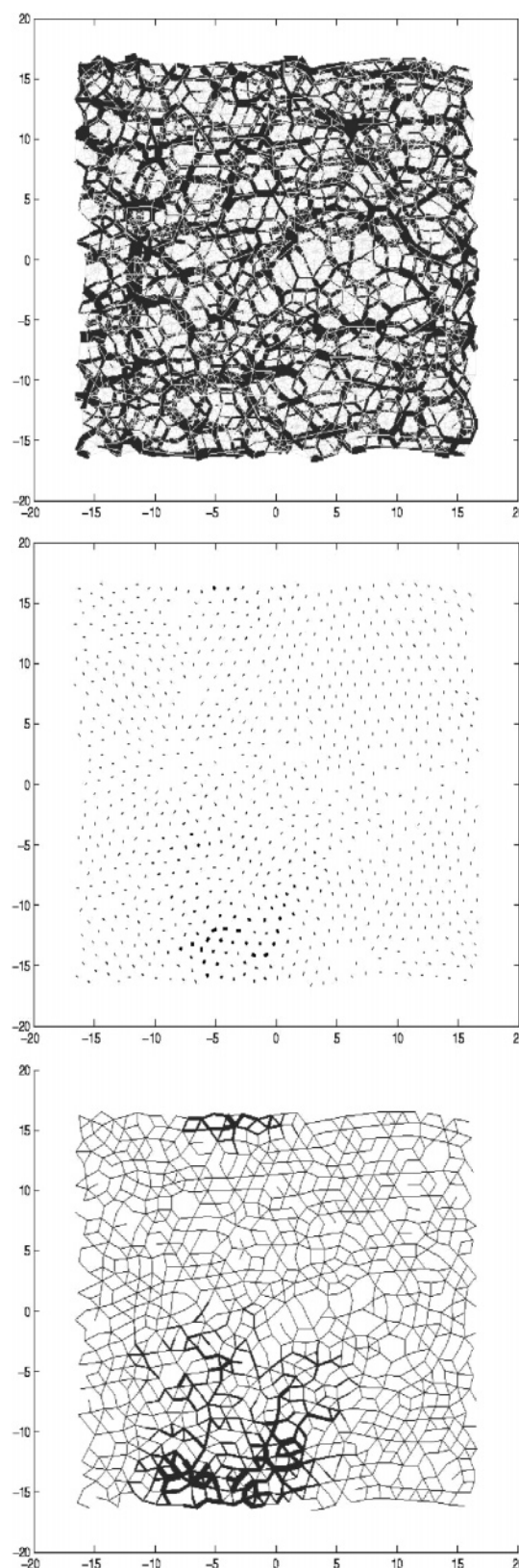


**Figure 8.** (a) Force network in an inherent structure in the polydisperse LJ liquid at  $T = 1$ . Each line connects two particles and represents the repulsive force between them. The thickness of the lines are proportional to the magnitude of the forces. (b) Particle displacements during an inherent structure transition in the polydisperse LJ liquid at  $T = 1.0$ . The size of the lines are proportional to the magnitude of the displacement. (c) Changes in forces during an inherent structure transition in the polydisperse LJ liquid at  $T = 1.0$ . The size of the lines are proportional to the magnitude of the change in the forces.



Kob–Andersen liquid does not show a finite force peak and instead shows an exponential distribution like the equilibrated liquid. Further, we do not find any evidence of a lack of self-averaging in the force distribution. On the other hand, the two-dimensional binary soft sphere system displays a finite force peak in equilibrium. This observation, in conjunction with the known “strong” dynamical behavior of this system, leads us to speculate that the force distributions may look qualitatively different for strong liquids. Silicon and silica, which show strong behavior, display features in the force distributions previously attributed to jammed states and further display considerably richer force distributions than seen in other systems previously. These cases lend support to the idea that force distributions may be correlated with the fragility of the liquids in question. However, the correlation is not entirely clear at present and would require further work to elucidate the precise relationship between fragility and the features seen in  $P(f)$ .

The behavior of inherent structures to a shear strain  $\gamma$ , on the other hand, shows a clear connection with the onset of slow dynamics. The exact reason for the observed connection needs to be better understood. Taken together with the gradual dependence of  $P(f)$  for inherent structures measured as a function of temperature, the sharp change in the critical value of  $\gamma$  needed to melt an inherent structure implies that  $P(f)$  alone cannot be sensitive to the yielding properties of glasses themselves, even if the transition from a liquid to a glass might be grossly indicated by the behavior of  $P(f)$  at small  $f$ .

Last, a preliminary study of force networks and force changes during inherent structure transitions has been presented here. More detailed studies of such behavior may be useful in understanding spatially heterogeneous dynamics and length scales relevant to the slow of dynamics in glass forming liquids, as well as elastic heterogeneity in glasses. This issue, as well as the resolution of several open questions raised in the previous sections of this work is the subject of ongoing investigation.

**Acknowledgment.** We thank C. S. O’Hern, A. J. Liu, S. R. Nagel, N. Menon, I. Saika-Voivod, J. Horbach, and W. Kob for useful discussions. We thank W. Kob, T. Schroeder, and R. Yamamoto for providing configurations for silica, 50:50 binary Lennard-Jones, and 2D soft spheres, respectively, and Budhadipta Dan for help with some of the calculations. D.R.R. and Y.B. thank NSF for financial support.

## References and Notes

- (1) Ediger, M. D.; Angell, C. A.; Nagel, S. R. *J. Phys. Chem.* **1996**, *100*, 13200.
- (2) Kauzmann, W. *Chem. Rev.* **1948**, *43*, 219.
- (3) Gibbs, J. H.; Di Marzio, E. A. *J. Chem. Phys.* **1958**, *28*, 373.
- (4) Adam, G.; Gibbs, J. H. *J. Chem. Phys.* **1965**, *39*, 139.
- (5) Kirkpatrick, T. R.; Thirumalai, D.; Wolynes, P. G. *Phys. Rev. A* **1989**, *40*, 1045.
- (6) Xia, X. Y.; Wolynes, P. G. *Proc. Natl. Acad. Sci. U.S.A.* **2000**, *97*, 2990.
- (7) Mezard, M.; Parisi, G. *J. Chem. Phys.* **1999**, *111*, 1076.
- (8) Götze, W.; Sjögren, L. *Rep. Prog. Phys.* **1992**, *55*, 241.
- (9) Fredrickson, G. H.; Andersen, H. C. *Phys. Rev. Lett.* **1984**, *53*, 1244.
- (10) Jäckle, J.; Eisinger, S. *Z. Phys. B* **1991**, *84*, 115.
- (11) Ritort, F.; Sollich, P. *Adv. Phys.* **2003**, *52*, 219.
- (12) Garrahan, J. P.; Chandler, D. *Phys. Rev. Lett.* **2002**, *89*, 035704.
- (13) Nagel, S. R.; Liu, A. J. *Nature* **1998**, *396*, 21.
- (14) Trappe, V.; Prasad, V.; Cipelletti, L.; Segre, P. N.; Weitz, D. A. *Nature* **2001**, *411*, 772.
- (15) Yamamoto, R.; Onuki, A. *Phys. Rev. E* **1998**, *58*, 3515.
- (16) Berthier, L.; Barrat, J.-L. *J. Chem. Phys.* **2002**, *116*, 6228.
- (17) Ono, I. K.; O’Hern, C. S.; Durian, D. J.; Langer, S. A.; Liu, A. J.; Nagel, S. R. *Phys. Rev. Lett.* **2002**, *89*, 095703.
- (18) Jaeger, H. M.; Nagel, S. R.; Behringer, R. P. *Rev. Mod. Phys.* **1996**, *68*, 1259.
- (19) Liu, C.-h.; et al. *Science* **1995**, *269*, 513.
- (20) Coppersmith, S. N.; et al. *Phys. Rev. E* **1996**, *53*, 4673.
- (21) Makse, H. A.; Johnson, D. L.; Schwartz, L. M. *Phys. Rev. Lett.* **2000**, *84*, 4160.
- (22) O’Hern, C. S.; Langer, S. A.; Liu, A. J.; Nagel, S. R. *Phys. Rev. Lett.* **2001**, *86*, 111.
- (23) O’Hern, C. S.; Langer, S. A.; Liu, A. J.; Nagel, S. R. *Phys. Rev. Lett.* **2002**, *88*, 075507.
- (24) O’Hern, C. S.; Silbert, L. E.; Liu, A. J.; Nagel, S. R. *Phys. Rev. E* **2003**, *68*, 011306.
- (25) See, also: Lacks, D. J. *Phys. Rev. Lett.* **2001**, *87*, 225502. In this paper a connection is made with the mode-coupling temperature and not the onset temperature.
- (26) Kob, W.; Andersen, H. C. *Phys. Rev. E* **1995**, *51*, 4626. Vollmayr, K.; Kob, W.; Binder, K. *J. Chem. Phys.* **1996**, *105*, 4714.
- (27) Sastry, S.; Debenedetti, P. G.; Stillinger, F. H. *Nature* **1998**, *393*, 554.
- (28) Sastry, S. *PhysChemComm* **2000**, 14.
- (29) Schröder, T. B.; Sastry, S.; Dyre, J.; Glotzer, S. C. *J. Chem. Phys.* **2000**, *112*, 9834.
- (30) Tanguy, A.; et al. *Phys. Rev. B* **2002**, *66*, 174205.
- (31) Brumer, Y. Ph.D. thesis, Harvard University (unpublished).
- (32) Stillinger, F. H.; Weber, T. A. *Phys. Rev. B* **1985**, *31*, 5262.
- (33) Sastry, S.; Angell, C. A. *Nature Mater.* **2003**, *2*, 739.
- (34) Angell, C. A.; et al. *Phys. Chem. Chem. Phys.* **2000**, *2*, 1559.
- (35) van Beest, B. W. H.; et al. *Phys. Rev. Lett.* **1990**, *64*, 1955.
- (36) Scheidler, P.; Kob, W.; Latz, A.; Horbach, J.; Binder, K. *Phys. Rev. B* **2001**, *63*, 104204.
- (37) Angell, C. A.; Ngai, K. L.; McKenna, G. B.; McMillan, P. F.; Martin, S. W. *J. Appl. Phys.* **2000**, *88*, 3113.
- (38) Horbach, J.; Kob, W.; Binder, K. *Eur. Phys. J. B* **2001**, *19*, 531.
- (39) Horbach, J.; Kob, W. *Phys. Rev. B* **1999**, *60*, 3169.
- (40) Ashwin, S. S.; Sastry, S. *J. Phys. Condens. Mater.* **2003**, *15*, S1253.
- (41) Evidence that the 50:50 soft-sphere mixture has some features of a strong liquid comes from three sources. First, the self-intermediate scattering function  $F_s(k, t)$  shows marked short-time oscillations characteristic of strong liquids.<sup>38,42</sup> Although it is known that the strength of such oscillations is dependent on system size,<sup>43</sup> the appearance of such behavior at all is indicative of strong behavior. Second, the 50:50 soft-sphere mixture shows marked finite size effects in the  $\alpha$  relaxation time<sup>44</sup> that is expected for strong liquids.<sup>45</sup> Last, the ratio of the  $T_c$  of mode-coupling theory<sup>46</sup> to the expected ideal glass transition temperature  $T_K$  where an entropy crisis would occur in the mean-field limit<sup>47</sup> is large for the 50:50 soft-sphere mixture compared to the more fragile BMLJ system of Kob and Andersen.<sup>48</sup> This is consistent with strong behavior on the fragility scale.
- (42) Perera, D. N.; Harrowell, P. *Phys. Rev. E* **1999**, *59*, 5721.
- (43) Muranaka, T.; Hiwatari, Y. *Phys. Rev. E* **1995**, *51*, R2735.
- (44) Kim, K.; Yamamoto, R. *Phys. Rev. E* **2000**, *61*, R41.
- (45) Horbach, J.; Kob, W.; Binder, K.; Angell, C. A. *Phys. Rev. E* **1996**, *54*, R5897.
- (46) Grigera, T. S.; Cavagna, A.; Giardinà, I.; Parisi, G. *Phys. Rev. Lett.* **2002**, *88*, 055502.
- (47) Coluzzi, B.; Mezard, M.; Parisi, G.; Verrocchio, P. *J. Chem. Phys.* **1999**, *111*, 9039.
- (48) Coluzzi, B.; Parisi, G.; Verrocchio, P. *J. Chem. Phys.* **2000**, *112*, 2933.
- (49) In addition to two-body interactions, the Stillinger–Weber potential includes a sum over three-body terms of the form  $U_3(\mathbf{r}_i, \mathbf{r}_j, \mathbf{r}_k)$ . The  $\alpha$ th component of the total force on a given atom  $i$  can be written as,

$$F_{i,\alpha} = - \sum_{j,k} \frac{\partial U_3(\mathbf{r}_i, \mathbf{r}_j, \mathbf{r}_k)}{\partial r_{i,\alpha}} \equiv \sum_j F_{ij,\alpha}$$

where the second step defines what we consider to be “pairwise” forces between  $i$  and  $j$ , arising from three body interactions.

(50) Wittmer, J. P.; Tanguy, A.; Barrat, J. L.; Lewis, L. *Europhys. Lett.* **2002**, *57*, 423.

(51) Tanguy, A.; Wittmer, J. P.; Leonforte, F.; L. Barrat, J. *Phys. Rev. B* **2002**, *66*, 174205.